Environmental impact investigation on the interlaminar properties of carbon fibre composites modified with graphene nanoparticles.

W. Jarrett[*], F. Korkees[**]

[*]Institute of Structural Materials, College of Engineering, Bay Campus, Swansea University, Swansea, SA1 8EN, UK, 901379@swansea.ac.uk, +447818518293.

[**] Engineering East, College of Engineering, Bay Campus, Swansea University, Swansea, SA1 8EN, UK, F.A.Korkees@swansea.ac.uk.

Abstract **–** Graphene nanoparticles have been widely studied for their all-round promising positive effects. In this study, the effect of adding functionalised 2% NH2-graphene nanoparticles to carbon fibre/epoxy composite was assessed, before and after hygrothermal and ultraviolet exposure. The interlaminar shear strength and glass transition temperature of the filled and unfilled were experimentally determined, after being immersed in water at 25°C, 40°C and 70°C until partially saturated. Other samples were exposed to ultraviolet for 700 and 1400 hours. With graphene, samples showed up to 43.9% better water uptake resistance. The interlaminar shear strength decreased after immersion in water by an average of 5.8% with graphene, however, after ultraviolet exposure the ILSS loss commonly attributed to UV exposure was reduced by 12.1% with graphene. This improvement can be explained by the GNPs offering stability against free-radical ageing, slowing the rate of scissions and the eventual transformation to constituent monomers. Dynamical mechanical analysis on immersed samples showed that the graphene reduced glass transition temperature by only 1%. Filled samples exposed to UV for 1400 hours suggested a reduction in glass transition temperature of 1°C. Scanning electron microscopy revealed good dispersion of the GNPs in the epoxy matrix but with no strong bonding.

Keywords: Nano composites; Nano particles; Hygro-thermal effect; Interfacial strength; Dynamic mechanical thermal analysis (DMTA)

1. Introduction

The Engineering industry is constantly striving to find new, lightweight materials to provide alternatives to more conventional means of manufacturing. This leads to increased efficiency with less fuel being used to lift, for example, aircraft, where the Airbus A350 XWB has an airframe constituting 52% reinforced plastics [1], [2] such as carbon fibre reinforced polymers (CFRP), which this paper will focus on. To conceive a plausible weight saving option for CFRP could be valuable to not only the aerospace industry, but to all engineering disciplines that would benefit from weight saving techniques. For these new materials, it would be essential to test how well they resist common engineering environmental conditions, namely hot and wet and UV exposed, and how these compare with the original materials.

The use of graphene nanoparticles (GNPs) in CFRPs, which is carbon arranged in a hexagonal lattice with covalently bonded atoms [3], is of particular interest largely due to its superior strength; with a tensile strength of 130.5 GPa it is the strongest material ever tested [4]. This fact increases the likelihood that this material arranged in a nanoparticle format will be able to retain, at the least, the material's mechanical properties when dispersed correctly. To further the development of these CFRPs, these nanoparticles can be added to potentially enhance certain properties of the material, such as the interlaminar shear strength (ILSS), glass transition temperature (T_g) and water uptake rate, which this paper will mainly cover. This is important as, for example, the ILSS is a major factor contributing to the onset and propagation of delamination [5]. As the research of using GNPs in composites is still in its infancy, there are relatively few studies assessing how a CFRP with GNPs mechanical properties are affected by hygrothermal and UV exposure. This gap in the literature offers new research opportunities that will be addressed in this study.

The more general positive effects of adding reinforcing nanoparticles on a polymer composite's mechanical properties has been studied before [3], [6], with resounding fatigue and tensile strength improvements of 91.2 and 38.2% respectively. Here, assuming correct particle dispersion and matrix bonding, their improved mechanical properties were attributed by high levels of energy absorption and a positive influence on grain growth. Other particulate reinforcement can come in microscale, and their general mechanical property changes have been studied [7], [8] however in less depth than for nanoscale. This lack of research can be attributed to studies [9], [10] suggesting decreasing particle size in general leads to an improvement in the mechanical properties of the material. More specifically to this paper, numerous studies [11], [12], [13], [14] have shown the positive effects that nanoparticles have on the ILSS of composite materials. Using 0.3 % wt. graphene oxide, 0.5 % wt. carbon nanotubes, or 42 % matrix wt. nanosilica and 25 % matrix wt. core shell rubber respectively, ILSS had a range from 47.4 – 74.8 MPa, with percentage increases over standard CFRP of up to 102.9%. Here, the nanofillers were used to connect the epoxy and the fibres, creating a network of bridges that are used to share load and hence increase the ILSS. However one study [15] suggested a 3.14 and 12.21 % decrease after the inclusion of 10% wt. and 20 % wt. silica nanoparticles respectively.

UV damage to the epoxy can be a significant factor for composite failure, as shown by previous studies [16], [17], [18]. It is therefore important to limit this effect, and there are studies [19], [20] suggesting that nano-scale inclusions in the material may help. The latter study used graphene nanoplatelets incorporated in an epoxy film at between 0.1% and 1% by weight, and concluded that there was a strong decrease in damage and loss of mechanical properties. Ultraviolet light (UV) has shown to have the ability to increase the concentration of free radicals in a polymer, which then leads to degradation [18]. This is important as if the polymeric surface of the composite is degraded in this way, the fibres will be exposed, further increasing moisture absorption [21].

When determining the mechanical properties of a material after water absorption at differing temperatures, it is known as testing its hygrothermal capabilities. Many studies [22], [23], [24], [25]

have reported on the effects of immersing CFRPs and the corresponding diffusion, with [22] showing a 37% reduction in 90° tensile strain to failure in samples with 1% moisture content after immersion. A reduction in strength, stiffness and a change in fracture mode was also found in [23], with the severity of matrix cracking and delamination increasing with moisture content. These changes can, in part, be explained by reports [24], [26].

The interlaminar shear response is to be tested after prolonged immersion in water for over 1 month, simulating the potential change in humidity that an aircraft may be subject to. There are few relevant studies looking at how GNPs affect this hygrothermal capability, but one study does suggest that the strength of a composite without nanoparticles decreases above immersion at 70°C after testing a range from 20 to 130°C [27]. Furthermore, a study looking at hydrothermal ageing effects at room temperature [28] showed that composites with functionalised graphene oxide nanoparticles (1.72 wt.%) had a superior reinforcement efficiency after ageing, and lower water diffusivity (40%) and leaching effects (70%). There is still, however, a gap in research and an opportunity to compare the ILSS of an immersed carbon composite with and without GNPs at a range of temperatures. There has been some research into how graphene's presence in an epoxy slows the rate of water uptake. A study [29] showed that the use of graphene nanoplatelets reduces the absorbed moisture content. Furthermore, it is suggested that maximum water content and diffusion coefficients are decreased. This opens potential research covered in this study to assess GNPs effectiveness in these areas.

When assessing how the addition of GNPs, in general, affect the T_g, a study suggests that incorporating graphene up to 1.5 wt.% resulted in an epoxy stiffness increase. This in turn led to a significant increase in T_g of 40°C [30]. In this case, the dispersion of the graphene was a success, with particles uniformly dispersed and fully embedded. Whilst there are not many relevant studies assessing GNPs effect on T_g after hygrothermal exposure, one study suggests that the T_g of a carbon fibre composite was observed to reduce by about 17% due to being hygrothermally aged in a chamber at 70°C and 85% relative humidity [31]. This effect will be assessed in this study, whilst also filling the knowledge gap of how GNPs can effect this change in T_g.

The technique used in this project aims to reduce carbon fibre density in the material, and instead partially replace them with graphene nanoparticles (GNPs). The hypothesis is that through the process of functionalization, where the GNPs are evenly spread throughout the resin, they can act as a load bearer, while also providing obstacles for dislocations and crack propagation, and hence slow the rate of fatigue induced damage – a process common, for example, in an aircraft's repetitive lifecycle. Therefore, the outcome is a material that theoretically provides increased interlaminar shear strength, reduced weight compared with conventional CFRPs and the added characteristic of having a significantly increased service life [3]. Furthermore, the rate of absorption was measured for both materials to assess how GNPs and temperature affect the long-term moisture uptake of the CFRPs. The hypothesis here is that the introduction of GNPs will hinder the path of the water molecules and hence slow the uptake. T_g was determined to study the effect that water and temperature have on it, using Dynamic Mechanical Analysis (DMA). This is important as beyond this transition temperature, the material may become more flexible with the presence of water molecules. In general, the hypothesis is that with the presence of GNPs, ILSS and T_g will increase after hygrothermal and UV exposure, and the water uptake rate will slow. The results will then be ratified using SEM imaging, assessing the dispersion and bonding of the GNPs in the matrix.

2. Materials and Methods

The material tested in this study is carbon fibre/epoxy composite reinforced with 2% NH2-GNPs. It used a 2x2 twill carbon fibre woven fabric of 0.28mm thickness and orientation [0, 90], with each fibre having a 7 µm filament diameter, and tensile strength 4120 MPa. Furthermore, it used an IN2 epoxy infused resin, where the tensile strength was between 63.5 – 73.5 MPa, and T_g onset was 92-98°C. Both fibres and epoxy were supplied by Easy composites. The nanoparticles used were oxygen functionalised graphene nanoparticles with a surface area of 500 $m^2 \cdot g^{-1}$ provided by Perpetuus Carbon Technologies Ltd. Amine-GNPs contained the amine functional group, consisting of basic nitrogen atoms, which are able to hydrogen bond with other hydroxyl groups, hydrogen atoms and

molecule [32]. They were prepared using plasma-processing in a multi-electrode dielectric barrier discharge plasma reactor [33]. Here, the graphite powders are exposed in an argon plasma for 60 minutes at 3 and 6 kW. This exfoliates the graphite and negates the van der Waals forces between the layers. Oxygen plasma is then used to introduce O_2 functional groups to reducing agglomeration [34]. The 2% amine GNPs were first mixed with epoxy using shear mixing and a three-roll mills mixer. The composite panels were then manufactured by resin infusion moulding. The sheets were cured first at room temperature using UV lights for 24 hours followed by 6 hours curing in an oven at 60°C.

Samples were cut using a waterjet into approximately 20mm length, 10mm width, and 2mm thickness. They were first dried in an oven at 70°C with desiccants and weighed periodically until the sample weights stabilised. Fifteen samples of each material were then immersed in distilled water at different temperatures 25°C, 40°C, and 70°C. The weight of the samples was monitored periodically until saturation. The percentage weight gain, W_g%, was calculated using equation (1).

$$W_g\% = \frac{W_t - W_o}{W_o} \cdot 100 \quad (1)$$

Where, W_t is the weight measured after immersion at a time t, and W_o is the initial weight before immersion.

Ten samples of each material were also subjected to UV radiation in a QUV accelerated weathering tester using UVA lights. Half of the samples of both materials were removed and tested after 700 hours and 1400 hours.

For the interlaminar response of the material, short beam shear testing was used with a Hounsfield testing machine (Figure 1), and all procedures followed BS 2563. This method is based on classical beam theory, and causes transverse shear failure through three point bending, a method that also

allows easy comparison to other studies [12], [13]. The samples were placed in the shear holder, with the span width set to 10mm according to equation (2).

$$\boldsymbol{Iv = 5 \cdot \bar{h} \pm 0.1} \quad (2)$$

The strain rate was then set to 1mm·min^{-1} and programmed to record load every 0.2 seconds. The maximum shear strength was determined using equation 3.

$$\boldsymbol{T = \frac{3 \cdot PV}{4 \cdot b \cdot h}} \quad (3)$$

Where, *PV* represents the maximum load at the moment of first failure (N); *b* represents the width of the specimen (mm); *h* represents the thickness of the specimen (mm). This ILSS was calculated in the longitudinal orientation, that is the crack propagation is perpendicular to the fibres.

Figure 1: A sample during ILSS testing on Hounsfield tester

DMA testing was performed to determine how GNPs affect T_g in several conditioning environments: without environmental consideration, after immersion in water at different temperatures, and

exposure to UV light. Two immersed samples of each material from the temperatures 25°, 40° and 70° were tested, along with one UV exposed sample from each material at both 700 hours and 1400 hours. A Perkin Elmer 8000 DMA was used with a single cantilever to determine the glass transition temperature T_g, and all procedures followed ISO 6721. The samples were heated up to 160°C at 5°C/min. The frequency used was 1 Hz and at 0.03% strain. The samples were placed in the machine, and two samples of each were tested.

A Crossbeam 540 FIB-SEM by Zeiss was used to evaluate the dispersion and bonding of the GNPs to the matrix. The samples were prepared, and sputter coated in 5nm of platinum to avoid charging on the SEM. This conductive layer of metal increases the number of secondary electrons that can be detected, leading to an improved signal to noise ratio. This process also leads to a reduced beam penetration which has the effect of improving edge resolution [35].

3. Results and Discussion

3.1. Water Uptake

Error! Reference source not found. showing water uptake rate shows that the absorption seen here is lower than that seen in other studies on nanoparticle reinforced epoxy composites [36], [37] that show water uptake up to 6%. This can be explained to be from the presence of the carbon fibres and the higher crosslinking in higher grade epoxies [29]. The weight gain initially followed Fickian behaviour, where there exists a linear relationship between average weight gain and the square root of time. After this, however, there is evidence of a longer-term, second-stage absorption as the weight gain continues to increase past the linear section. Studies by Korkees et al [25], [38] explains this could have been due to polymer chain relaxation, where the absorbed water in all samples is believed to induce structural relaxation in the resin, allowing water molecules to take up any new space. Other studies [39], [40] also explain the two-stage water uptake trend with resin relaxation.

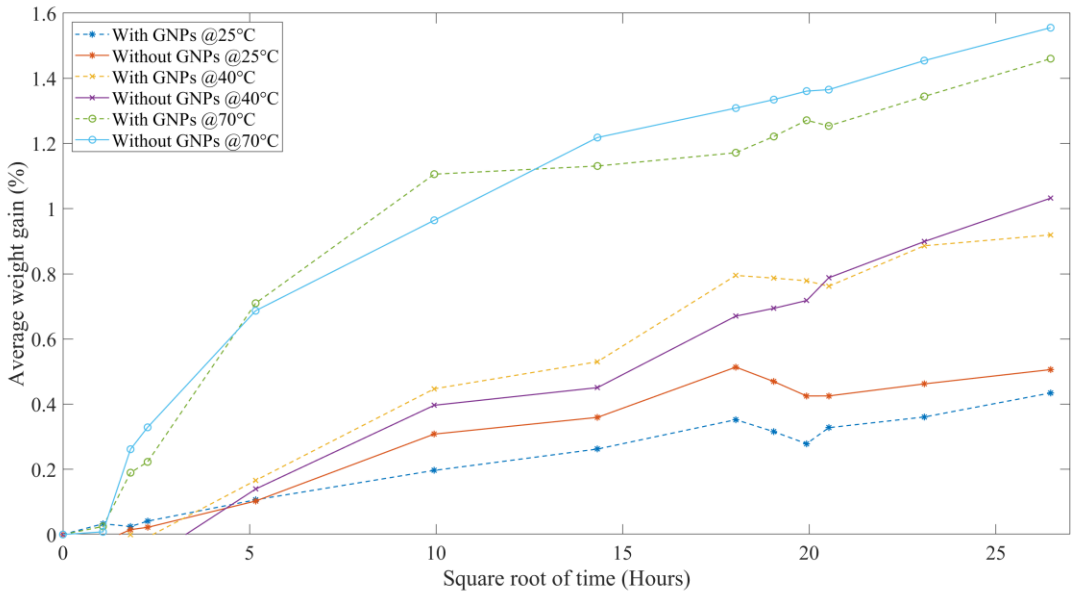

Figure 2: Water uptake curves for specimens in water at 25°C, 40°C and 70°C against the square root of time

Therefore, a graphical method [38] can separate the Fickian and long-term behaviour and be used to come to a new maximum moisture content, M_f, which coincides with the theoretical Fickian diffusion curve maximum, figure 3. As an example, with GNP at 70°C is shown, and was also applied to all curves at the various temperatures and compositions.

After M_f values were obtained, the gradient, *G*, of the initial half section (short term absorption) of the curve was calculated using equation (4). The diffusion coefficient, *D* was determined using equation (5).

$$\boldsymbol{G = \frac{Mt2 - Mt1}{\sqrt{t2} - \sqrt{t1}}} \tag{4}$$

$$\boldsymbol{D = \frac{\pi \cdot G^2 \cdot h^2}{16 \cdot {M_f}^2}} \tag{5}$$

Where *h* is the thickness of the sample. The D values are calculated using their respective gradients at each temperature and material.

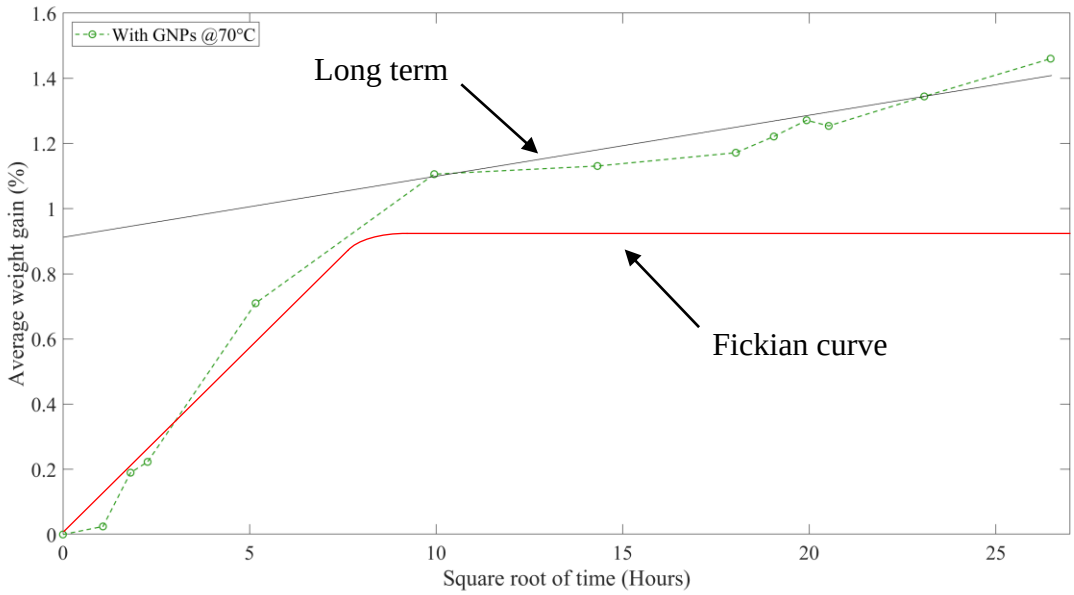

Figure 3: Water uptake curve for specimens in water at 70°c with extracted Fickian behaviour from long term measurements

As mentioned, the initial uptake (Figure 2) of both materials at 70°C follows Fickian behaviour, followed by a brief period of early saturation levelling and then a progression to long term absorption. The 25°C and 40°C samples show less Fickian behaviour (Figure 2), with less of the characteristic initial uptake as well as not levelling off as clearly. For this study, the maximum moisture content, M_f, will be taken at the longest time possible. This assumes the curves level off soon after. Using the equations (4) and (5), the average diffusion coefficients were determined from table 1, and presented showing a decrease in the diffusion coefficient at each temperature with the presence of GNPs (Figure 4). The results suggest that beyond 40°C, an increase in temperature led to an increase in coefficient, found also in [38]. This agrees with [24] that suggests diffusion is a thermo-active process, that's sensitive to temperature of immersion, and related to the Arrhenius equation, which suggests that increasing the temperature accelerates short term diffusion.

GNPs did show some sign of beneficial physical behaviour. They decreased the diffusion coefficients markedly at 70°C (Figure 4), a result directly leading from a slower water uptake, and reduced the maximum water content. The reasons for the increase of water resistance due to GNPs

can be summarised by the GNPs acting as barriers against water absorption and impairing the intermolecular movements of the surrounding epoxy. A similar effect can be seen in [41]; carbon nanotubes gave a 20-30% decrease in water uptake rate compared to without, citing the same cause as above but also suggesting the formation of strong chemical interfaces between the epoxy matrix and amine-functionalised carbon nanotubes, hindering water molecule diffusion further. Here, any primary crack induced by a temperature rise has the nonreinforcements as an obstacle, increasing the energy required for local crack deviations. The diffusion decreasing affect was found also by [24] where the addition of carbon fibres to resin reduced the diffusion values, and so the presence of fibres may have hindered water movements through the resin by constraining polymer chain movement. The same argument was used by [42], showing rigid carbon fibres may constrain matrix movement.

Table 1: A table showing the Mf and corresponding D values

Samples	Mf %	D (10^-14m^2/s)
25°C With GNPs 1	0.41	3.0814
25°C With GNPs 2	0.46	2.4479
25°C Without GNPs 1	0.49	3.0132
25°C Without GNPs 2	0.52	3.1030
40°C With GNPs 1	0.89	3.4684
40°C With GNPs 2	0.95	2.964572368
40°C Without GNPs 1	0.94	3.445172778
40°C Without GNPs 2	1.13	3.725030673
70°C With GNPs 1	0.78	19.29190959
70°C With GNPs 2	0.76	18.91154855
70°C Without GNPs 1	0.88	35.45258706
70°C Without GNPs 2	0.86	32.69259021

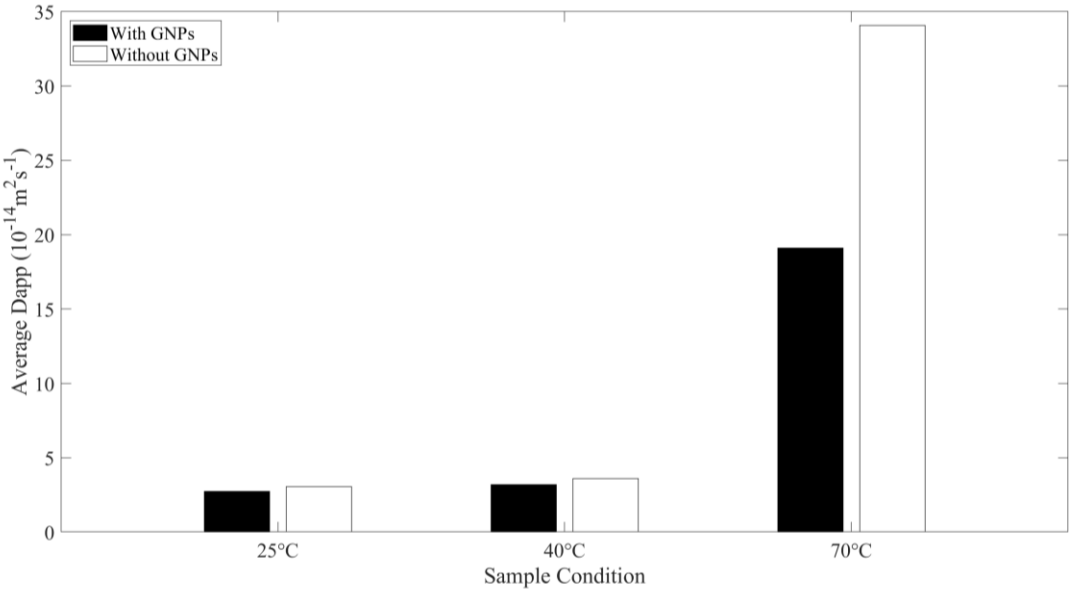

Figure 4: Average diffusion coefficient determined from gradient and maximum moisture content

3.2. Interlaminar Shear Test

ILSS tests were undertaken before immersion and UV exposure, to determine the normal comparison between the two materials, without environmental intervention (Figure 5). Specimens with and without GNPs followed the same ductile behaviour to failure, although the maximum loads that the material can withstand reduced slightly by the presence of GNPs. Figure 6 shows a decrease with GNPs in ILSS of 3.5%.

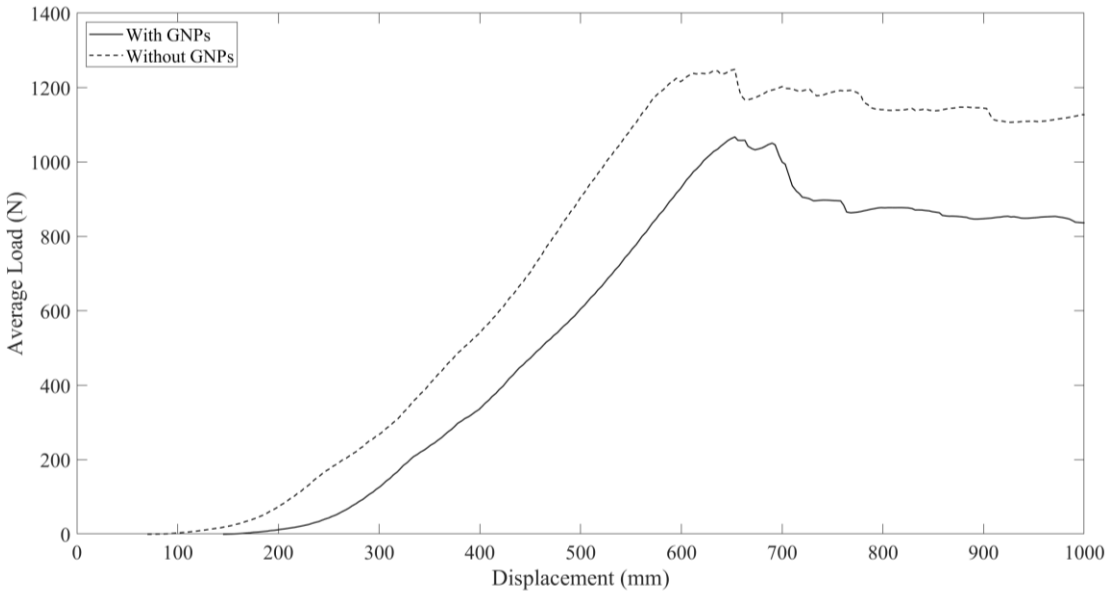

Figure 5: Average load against displacement (dry) – with and without GNPs - no environmental intervention

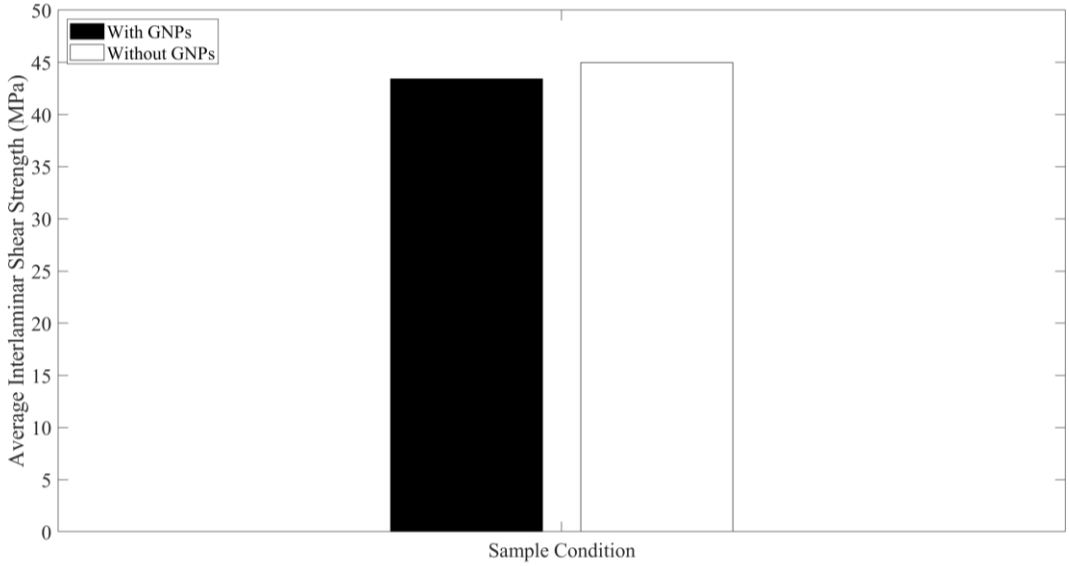

Figure 6: Average ILSS values for samples with and without GNPs - no environmental intervention

ILSS tests were also undertaken after the immersion in water at the three different temperatures. It can be shown that increasing the temperature at which the samples were immersed in, on average, reduced the load able to be withstood by the samples before failure, seen here by the peak. The results are in good agreement with [43] where the ILSS for CFRPs decreased after hygrothermal ageing while immersed at 70 and 85°C for 14 days by approximately 32% compared with the initial

state sample. This can be explained by heat mobilising chains in the polymer, allowing the greater diffusion of water into the material. This can then lead to matrix plasticisation, micro-cracking, and voids.

Furthermore, it can be seen (Figure 7) that GNPs affected the ILSS in a way that was not hypothesised, that is, the ILSS decreased at each temperature with the presence of GNPs, compared to without. An average percentage of how GNPs reduced the ILSS can be calculated to be 5.8%. The strength reduction seen after the inclusion of GNPs isn't unknown to literature, with Keledi et al [44] suggesting a reduction in tensile properties due to poor dispersion and/or adhesion/bonding. This would have led to easier delamination through stress concentrations building at the sites that have separated between mediums, thus leading to failure initiation. This is important as it can be shown that delamination causes reductions in ILSS, where the residual strength can be predicted from the area of delamination using a fracture mechanics model [45].

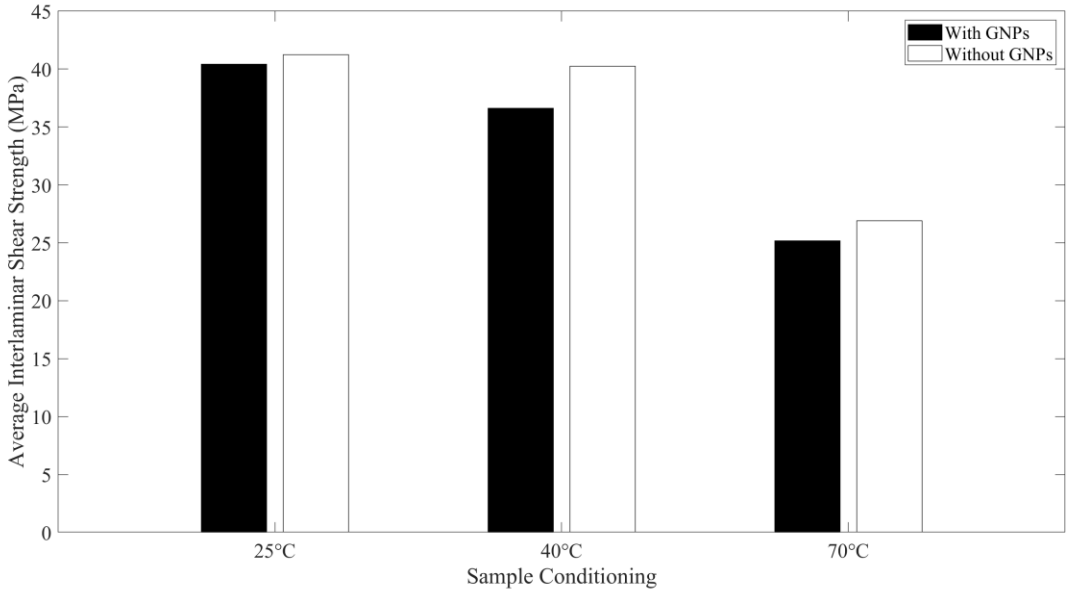

Figure 7: ILSS determined from pv and dimensions at 25°c, 40°c and 70°c – with and without GNPs – after immersion

A further ILSS test was performed on UV samples to access how the UV radiation affected the ILSS of the materials. The ILSS results (Figure 8) showed that the UV radiation exposure times had a minimal effect, but also showed that at both exposure times, the presence of GNPs gave a greater

resistance to a reduction in ILSS over the samples without GNPs when compared with their pre-exposure values. An introduction of GNPs in this case had a combined improvement of 12.1% when looking at ILSS loss resistance. This agrees with [46], that suggested the introduction of GNPs offers a decrease in the loss of mechanical properties. It is suggested [18] that UV radiation led photodegradation of the material, caused by free radicals. This secondary reaction relies on the availability of oxygen molecules in the matrix. Therefore, the improvement over composites without GNPs was likely due to the reduction in gas permeation through the polymer; the GNPs provided a 'tortuous path' that inhibited the gas diffusion in the matrix, reducing the oxygen availability. Another study [47] using carbon black nanoparticles, which have a similar composition to graphite, suggested that the nanoparticles acted as free radical 'scavengers', which help form peroxides that do not re-initiate oxidation reaction. Furthermore, it was suggested that the nanoparticles could have filled micro-pores in the epoxy, limiting water penetration that could accelerate UV degradation by improving mobility of free radicals.

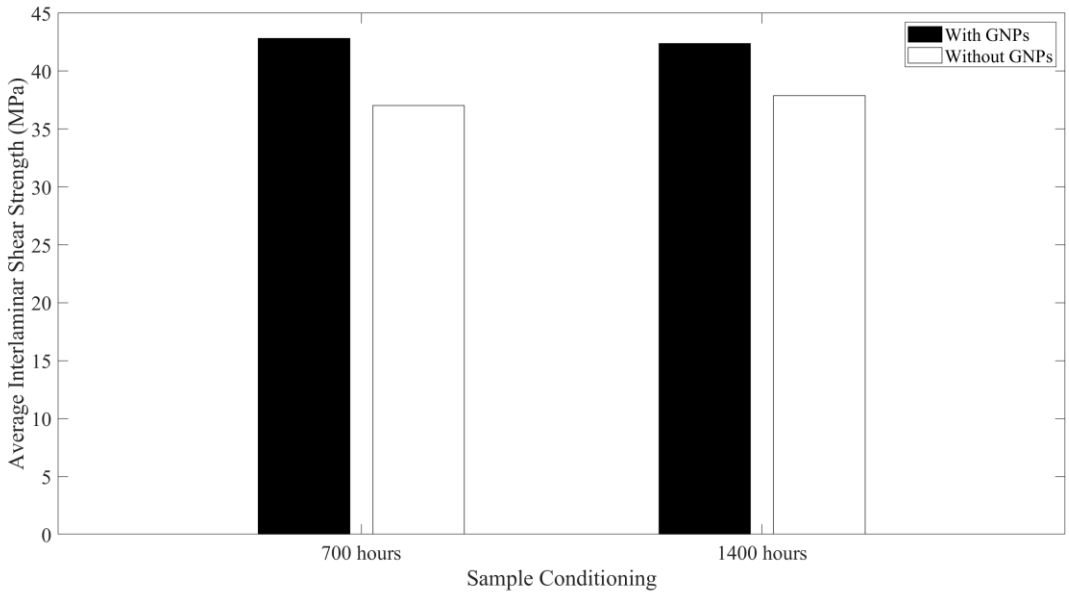

Figure 8: ILSS determined from pv and dimensions at 700 hours and 1400 hours UV exposure – with and without GNPs

3.3. Glass transition temperature

Figures 9 and 10 show the DMA graphs of GNP-filled and unfilled. The T_g is here determined by the tan delta peak, signified by a red dotted line. Across both materials, the T_g was highest at 25°C, with both 40°C and 70°C showing very similar reduced temperatures by an average of 11.1°C, or 13.4%. This reduction could have been due to the resin becoming increasingly plasticised, as it was shown that with increasing temperature, the water uptake increased.

The GNPs seem to have not affected the T_g substantially with it, on average, being reduced by 1.08% by the presence of GNPs. Due to the superior temperature capabilities of graphene nanoparticles, however, their introduction should be beneficial. For example, a study by Karthicksundar et al [48] attributed a 2°C increase in T_g to a 0.5% weight percentage nanofiller inclusion. The same study did show that nanoparticle inclusions higher than 0.5% led to a decrease in T_g, perhaps due to various reasons such as an increase in free volume from plasticisation, nanofillers interacting with the radius of gyration of the polymer chain, reducing the hindrance between atoms in the polymeric chain, and finally any impurities in the nanofiller. The T_g for both materials at each temperature is compared and shown (Figure 11).

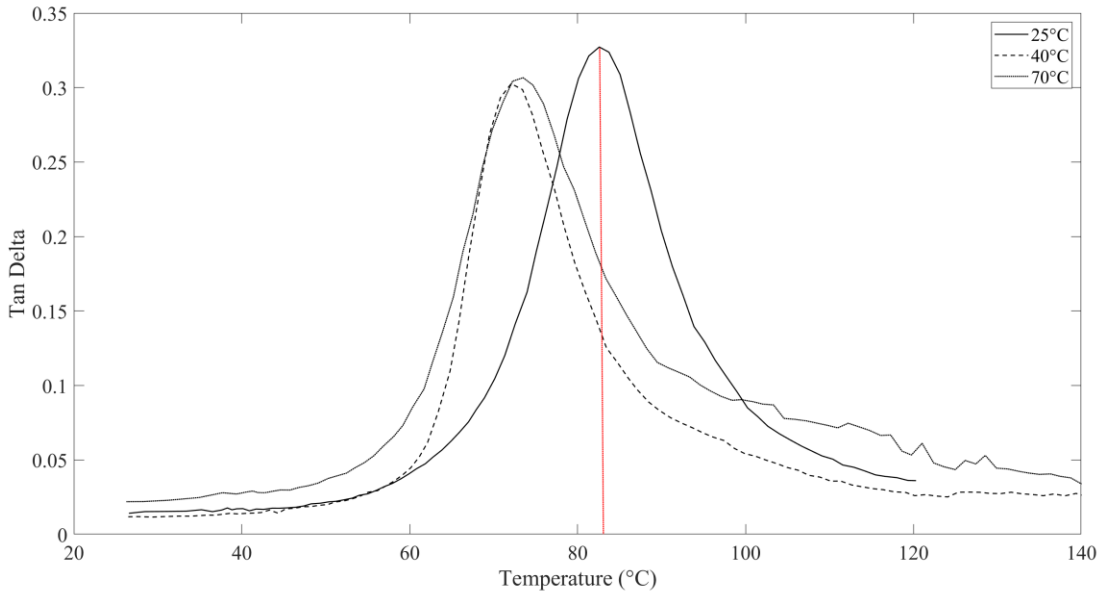

Figure 9: Tan delta against temperature at 25°c, 40°c and 70°c – with GNPs – after immersion

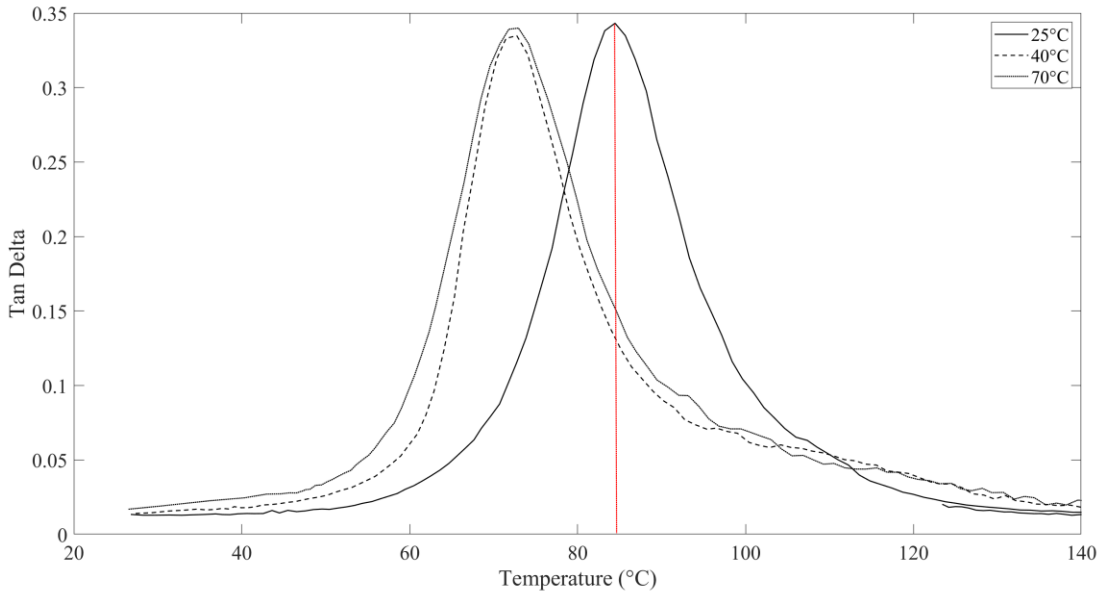

Figure 10: Tan delta against temperature at 25°c, 40°c and 70°c – without GNPs – after immersion

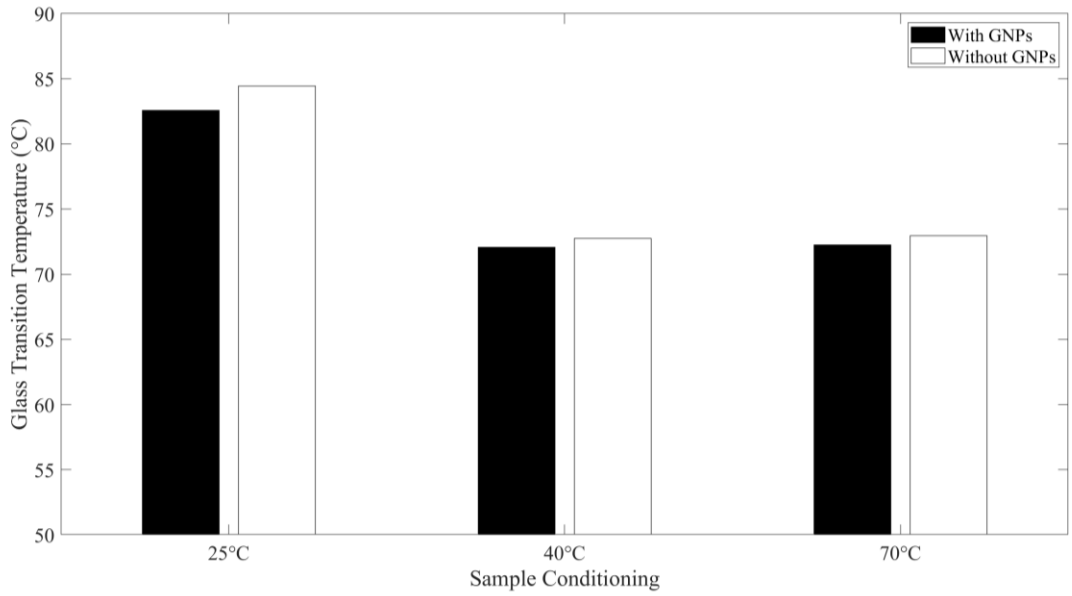

Figure 11: Glass transition temperatures at 25°c, 40°c and 70°c – with and without GNPs - after immersion

Further DMA was performed after exposure to UV, with the aim to compare how the introduction of GNPs affected the resultant T_g. Samples were tested having been exposed for 1400 hours (Figure 12). These results suggest a reduction in T_g of 1%, or 0.88°C with the introduction of

GNPs. This disagrees with the concept that as graphene absorbs the vast majority of the UV radiation [49], it should then release this as heat, post curing the material and increasing stiffness. The lack of correct particle/matrix bonding in this case may be the reasoning behind this.

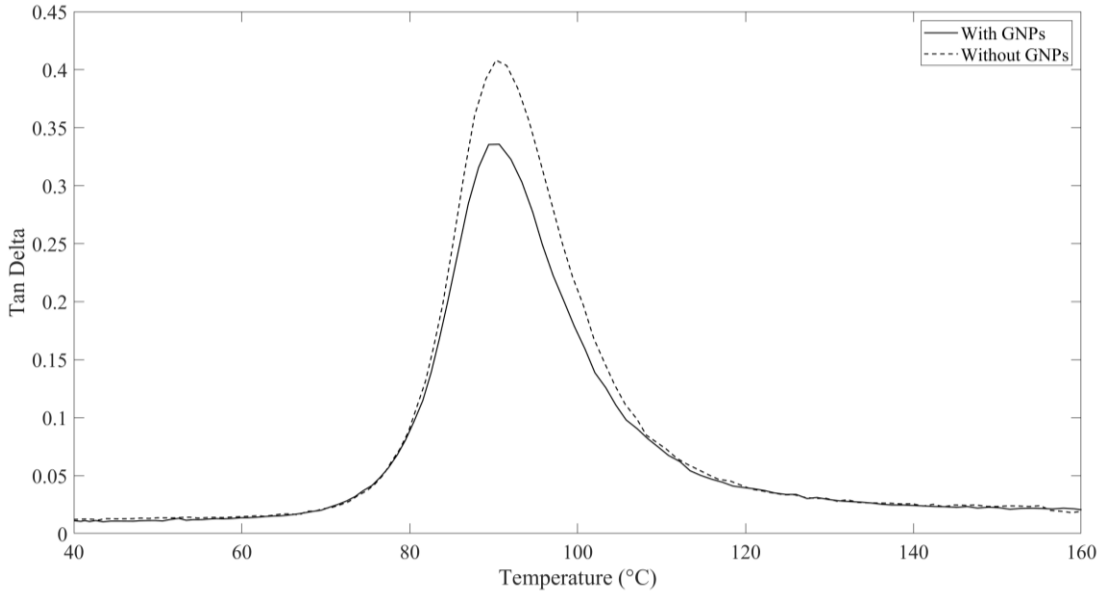

Figure 12: Tan delta against temperature after 1400 hours– with and without GNPs – after UV exposure

DMA was performed on a sample with zero environmental intervention, to measure the effect on the glass temperature after the sample was heated in the machine to 160°C, as was done on the samples. This is important to determine as the actual process of DMA may post cure the samples further creating a differing T_g when heating, than when cooling. This sample was post cured before this at 70° for seven days, as the aim was to try to have similar initial conditions as the other samples; they were seen to lose most of their moisture content after seven days. The results (Figure 13) suggest that the post curing effect of the heating reduces the T_g by 4.7°C, or more generally by 5%.

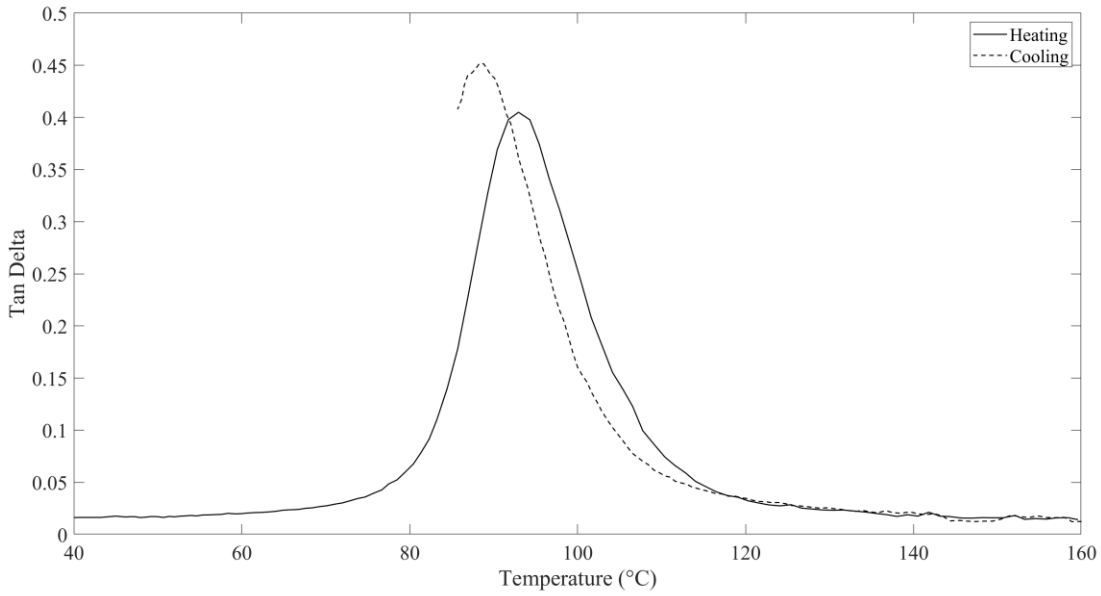

Figure 13: Tan delta against temperature after heating and cooling - zero intervention

3.4. Scanning Electron Microscopy

The GNPs gave the composite reduced mechanical properties such as ILSS when comparing with GNP inclusion and without both before environmental intervention and post immersion. To determine why this is the case, its microstructure was assessed visually using a SEM.

SEM was used to investigate the dispersion and bonding of GNPs to the matrix.
suggests that in practise, the dispersion was good and as intended with the lighter shaded spots shown by arrows highlighting the GNPs. As seen in [32], the functional groups O2 and Amine allowed the breaking of the van der Waal forces between the nanoparticles that would otherwise lead to agglomeration, and hence improving GNP immersion.

Furthermore, the bonding between the GNPs and the matrix was inspected, Figure 15. The microscopy image shows a poor bonding between the matrix and GNPs which can potentially lead to a reduction in the GNPs ability to share load and hence lead to no improvement in ILSS. The poor interfacial bonding is presented by the large, clean, and smooth GNP surface area shown without visible matrix attachment as in other studies on GNPs that showed improvement in material properties [32], [50] meaning it was not efficiently bonded to the matrix. A study [51] showed that

similarly flat, clean GNP surfaces could be seen, indicating very weak matrix interaction, resulting in debonding leading to microcracking under load, propagation, and eventual failure.

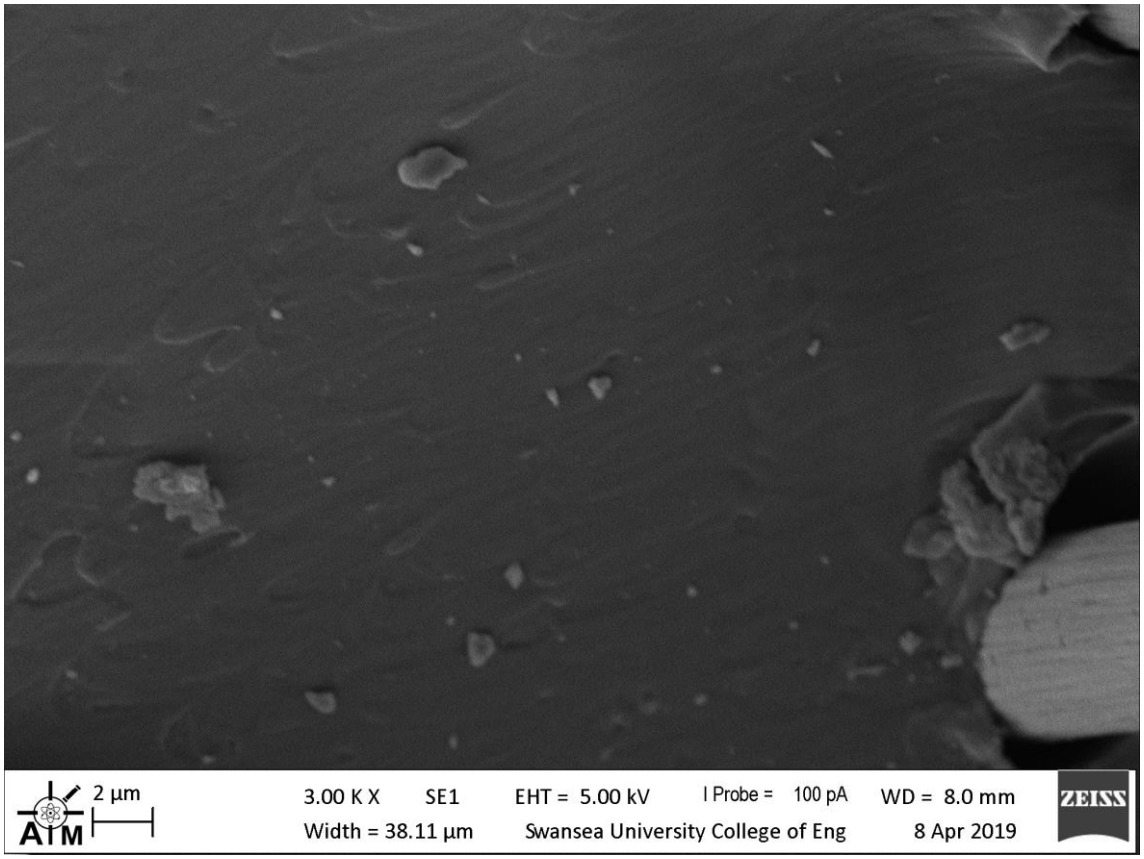

Figure 14: SEM image of dispersed GNPs in composite matrix

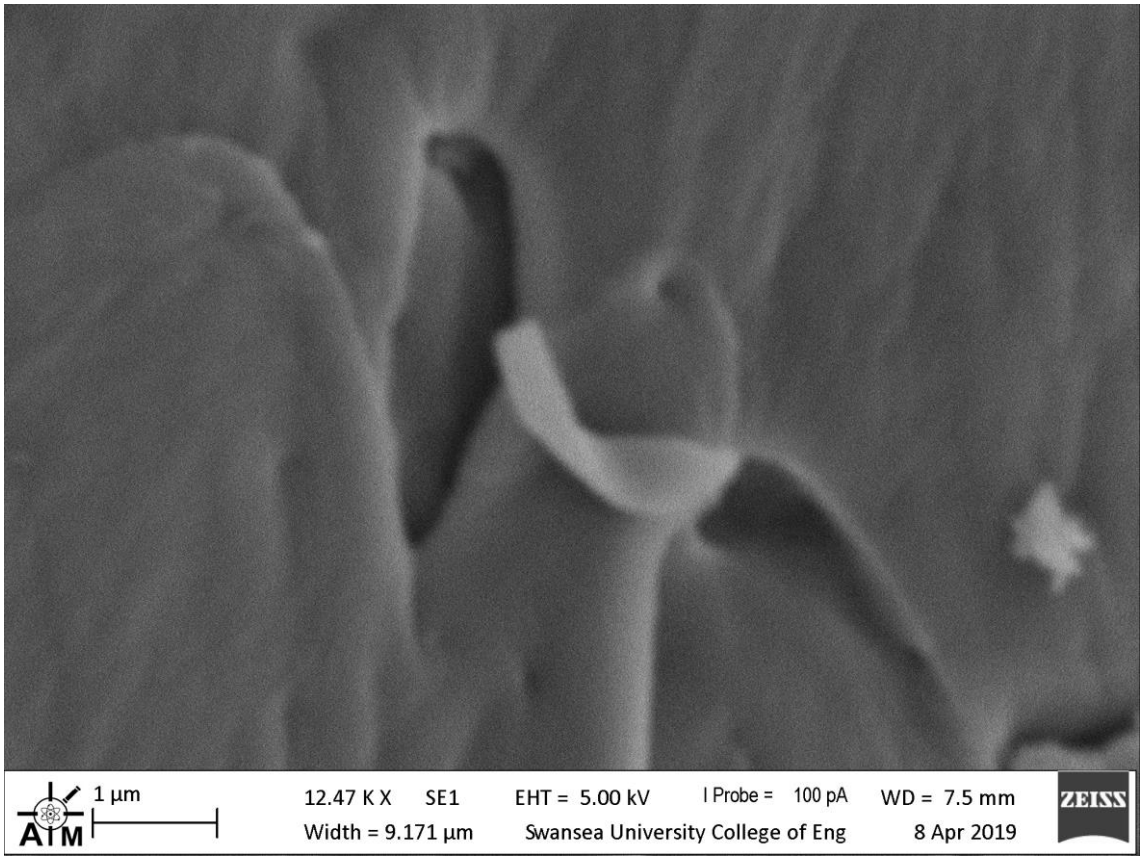

Figure 15: SEM image of GNPs incorrectly bonded in composite matrix

4. Conclusion

The purpose of the study was to examine the affect that adding graphene nanoparticles to a CFRP had on overall mechanical performance, both before and after environmental immersion. Through experimentation, it has been determined that the modification of carbon fibre composites with GNPs does change their mechanical properties.

The experiments involved the immersion of both composite samples in water at different temperatures for one month and exposure to UV radiation for 700 and 1400 hours. From this, the ILSS and T_g was determined for each condition and for each material, with and without GNPs. Furthermore, the rate of water uptake was compared between both materials, to determine how GNPs affected this.

Firstly, the study calculated the Fickian diffusion coefficient at each temperature and found that the coefficient decreased with the presence of GNPs, but significantly, at 70°C the water uptake was slowed by 43.9%.

Secondly, the study found GNPs to reduce the ILSS, for example, by a relatively small amount of 3.6%. Using scanning electron microscopy, this was attributed to incorrect bonding between the nanoparticles and the matrix; the images clearly show a large surface area of the GNP, proving the poor bonding between it and the matrix. This has potentially led to a reduction in the GNPs ability to share and distribute load with the matrix, and reduce their ability to divert cracks, hence leading to the reduction in strength.

Next, after immersion at 25°C, 40°C and 70°C and averaging the values across this range, the strength is measured to decrease by 5.8% after the introduction of GNPs. However, further testing suggested that after UV exposure, the interlaminar shear strength did not decrease nearly as much as the material without GNPs, with a significant loss improvement of 12.1%. This improvement could be explained by the reduction in gas permeation through the polymer. Other explanations involved the nanoparticles blocking free radical re-initiation and them acting as micro-pore fillers, slowing water uptake and hence UV degradation.

It was found that T_g was highest at 25°C by an average of 11.1°C. Both 40°C and 70°C showed very similar results, reducing the T_g in comparison to room temperature (25°C). This reduction was linked with some confidence to the higher temperatures increasing water uptake, and therefore increasing associated plasticization. The GNPs seem to have not affected the T_g substantially with it, on average, being reduced by 1.1% by the presence of GNPs, perhaps attributed to a higher than optimal percentage weight of nanoparticle.

Samples were tested after exposure to UV for 1400 hours. These results suggest a reduction in T_g of 1%, or 0.9°C with the introduction of GNPs.

Considering the beneficial water uptake and ILSS, UV characteristics of CFRPs modified with GNPs in this study, an engineering usage recommendation can be formulated for materials utilising

novel GNP/CFRP nanocomposite blends in the future. For example, it would be beneficial to use them in the aerospace, marine and automotive industries, where their hygrothermal and ultraviolet capabilities can potentially lead to safety, structural and economic improvements.

Acknowledgements

Thank you to Dr Feras Korkees for his work, significant help in the project and paper editing.

This research did not receive specific grants from funding agencies in the public, commercial, or not-for-profit sectors.

References

[1] J.-P. Immarigeon, R.T. Holt, A.K. Koul, L. Zhao, W. Wallace, J.C. Beddoes, Lightweight materials for aircraft applications, Mater. Charact. 35 (1995) 41–67. https://doi.org/10.1016/1044-5803(95)00066-6.

[2] G. Marsh, Airbus takes on Boeing with reinforced plastic A350 XWB, Reinf. Plast. 51 (2007). https://doi.org/10.1016/S0034-3617(07)70383-1.

[3] J.B. Knoll, B.T. Riecken, N. Kosmann, S. Chandrasekaran, K. Schulte, B. Fiedler, The effect of carbon nanoparticles on the fatigue performance of carbon fibre reinforced epoxy, Compos. Part A Appl. Sci. Manuf. 67 (2014) 233–240. https://doi.org/10.1016/j.compositesa.2014.08.022.

[4] C. Lee, X. Wei, J.W. Kysar, J. Hone, Measurement of the elastic properties and intrinsic strength of monolayer graphene, Science (80-.). 321 (2008) 385–388. https://doi.org/10.1126/science.1157996.

[5] D.J. Oehlers, I.S.T. Liu, R. Seracino, Shear deformation debonding of adhesively bonded plates,

Struct. <html_ent Glyph="@amp;" Ascii="&"/> Build. 158 (2005) 77–84. https://doi.org/10.1680/stbu.158.1.77.58531.

[6] M. Abu-Okail, N.A. Alsaleh, W.M. Farouk, A. Elsheikh, A. Abu-Oqail, Y.A. Abdelraouf, M.A. Ghafaar, Effect of dispersion of alumina nanoparticles and graphene nanoplatelets on microstructural and mechanical characteristics of hybrid carbon/glass fibers reinforced polymer composite, J. Mater. Res. Technol. 14 (2021) 2624–2637. https://doi.org/10.1016/j.jmrt.2021.07.158.

[7] N. Xu, C. Lu, T. Zheng, S. Qiu, Y. Liu, D. Zhang, D. Xiao, G. Liu, Enhanced mechanical properties of carbon fibre/epoxy composites via in situ coating-carbonisation of micron-sized sucrose particles on the fibre surface, Mater. Des. 200 (2021). https://doi.org/10.1016/j.matdes.2021.109458.

[8] D. Bharath, B. Sandhya Rani, V. Saritha, P. Irshad Khan, S. Kumar Chokka, Tensile and erosion behaviour of medium calcined alumina microparticles on GFRP composites fabricated with vacuum bagging process, Mater. Today Proc. 46 (2021) 307–310. https://doi.org/10.1016/j.matpr.2020.08.166.

[9] Y.M. Youssef, M.A. El-Sayed, Effect of reinforcement particle size and weight fraction on the mechanical properties of SiC particle reinforced al metal matrix composites, Int. Rev. Mech. Eng. 10 (2016) 261–265. https://doi.org/10.15866/ireme.v10i4.9509.

[10] P. Antil, S. Singh, A. Manna, Glass fibers/SiCp reinforced epoxy composites: Effect of environmental conditions, J. Compos. Mater. 52 (2018) 1253–1264. https://doi.org/10.1177/0021998317723448.

[11] X.J. Shen, L.X. Meng, Z.Y. Yan, C.J. Sun, Y.H. Ji, H.M. Xiao, S.Y. Fu, Improved cryogenic interlaminar shear strength of glass fabric/epoxy composites by graphene oxide, Compos. Part B Eng. 73 (2015) 126–131. https://doi.org/10.1016/j.compositesb.2014.12.023.

[12] K.C. Shekar, B.A. Prasad, N.E. Prasad, Interlaminar Shear Strength of Multi-walled Carbon Nanotube and Carbon Fiber Reinforced, Epoxy – Matrix Hybrid Composite, Procedia Mater. Sci. 6 (2014) 1336–1343. https://doi.org/10.1016/j.mspro.2014.07.112.

[13] Y. Wang, S.K. Raman Pillai, J. Che, M.B. Chan-Park, High Interlaminar Shear Strength Enhancement of Carbon Fiber/Epoxy Composite through Fiber- and Matrix-Anchored Carbon Nanotube Networks, ACS Appl. Mater. Interfaces. 9 (2017) 8960–8966. https://doi.org/10.1021/acsami.6b13197.

[14] J.J. Kim, A. Vashisth, C.E. Bakis, Testing of nanoparticle-toughened carbon/epoxy composites using the short beam strength method, 32nd Tech. Conf. Am. Soc. Compos. 2017. 4 (2017) 2708–2722. https://doi.org/10.12783/asc2017/15382.

[15] Y. Tang, L. Ye, D. Zhang, S. Deng, Characterization of transverse tensile, interlaminar shear and interlaminate fracture in CF/EP laminates with 10 wt% and 20 wt% silica nanoparticles in matrix resins, Compos. Part A Appl. Sci. Manuf. 42 (2011) 1943–1950. https://doi.org/10.1016/j.compositesa.2011.08.019.

[16] V.C. Malshe, G. Waghoo, Chalk resistant epoxy resins, Prog. Org. Coatings. 51 (2004) 172–180. https://doi.org/10.1016/j.porgcoat.2004.07.018.

[17] A. Rivaton, L. Moreau, J.L. Gardette, Photo-oxidation of phenoxy resins at long and short wavelengths - II. Mechanisms of formation of photoproducts, Polym. Degrad. Stab. 58 (1997) 333–339. https://doi.org/10.1016/S0141-3910(97)00088-8.

[18] A.P. Cysne Barbosa, A.P. Ana, E. S.S. Guerra, F. K. Arakaki, M. Tosatto, M.C. Maria, J.D. José, Accelerated aging effects on carbon fiber/epoxy composites, Compos. Part B Eng. 110 (2017) 298–306. https://doi.org/10.1016/j.compositesb.2016.11.004.

[19] H.R. Pakravan, H. Yari, The influence of nanostructured UV-blockers on mechanical properties of carbon fiber epoxy composites during accelerated weathering condition, Polym. Adv.

Technol. 29 (2018) 970–981. https://doi.org/10.1002/pat.4208.

[20] L. Guadagno, C. Naddeo, M. Raimondo, V. Speranza, R. Pantani, A. Acquesta, A. Carangelo, T. Monetta, UV irradiated graphene-based nanocomposites: Change in the mechanical properties by local harmoniX atomic force microscopy detection, Materials (Basel). 16 (2019). https://doi.org/10.3390/ma12060962.

[21] S. GS, Moisture content of composites under transient conditions, Composites. 9 (1978) 204. https://doi.org/10.1016/0010-4361(78)90355-5.

[22] Arnold JC, Alston S, Korkees F, Dauhoo S, Adams R, Older R, Design Optimisation of Carbon Fibre Epoxy Composites Operating in Humid Atmospheres, in: Compos. UK 10th Annu. Conf. Innov. Compos., 2010.

[23] F. Korkees, C. Arnold, S. Alston, Water absorption and low-energy impact and their role in the failure of ±45° carbon fibre composites, Polym. Compos. 39 (2018) 2771–2782. https://doi.org/10.1002/pc.24269.

[24] F. Korkees, S. Alston, C. Arnold, Directional diffusion of moisture into unidirectional carbon fiber/epoxy Composites: Experiments and modeling, Polym. Compos. 39 (2018) E2305–E2315. https://doi.org/10.1002/pc.24626.

[25] F. Korkees, R. Swart, I. Barsoum, Diffusion mechanism and properties of chemical liquids and their mixtures in 977-2 epoxy resin, Polym. Eng. Sci. 62 (2022) 1582–1592. https://doi.org/10.1002/pen.25946.

[26] C.E. Browning, The mechanisms of elevated temperature property losses in high performance structural epoxy resin matrix materials after exposures to high humidity environments, Polym. Eng. Sci. 18 (1978) 16–24. https://doi.org/10.1002/pen.760180104.

[27] O.M.K. Josh, The effect of moisture on the shear properties of carbon fibre composites, Composites. 14 (1983) 196–200.

[28] O. Starkova, S. Gaidukovs, O. Platnieks, A. Barkane, K. Garkusina, E. Palitis, L. Grase, Water absorption and hydrothermal ageing of epoxy adhesives reinforced with amino-functionalized graphene oxide nanoparticles, Polym. Degrad. Stab. 191 (2021). https://doi.org/10.1016/j.polymdegradstab.2021.109670.

[29] S.G. Prolongo, A. Jiménez-Suárez, R. Moriche, A. Ureña, Influence of thickness and lateral size of graphene nanoplatelets on water uptake in epoxy/graphene nanocomposites, Appl. Sci. 8 (2018). https://doi.org/10.3390/app8091550.

[30] M. Martin-Gallego, R. Verdejo, M.A. Lopez-Manchado, M. Sangermano, Epoxy-Graphene UV-cured nanocomposites, Polymer (Guildf). 52 (2011) 4664–4669. https://doi.org/10.1016/j.polymer.2011.08.039.

[31] A. Revathi, M.S. Murugan, S. Srihari, N. Jagannathan, C.M. Manjunatha, Effect of Hot-Wet Conditioning on the Mechanical and Thermal Properties of IM7/ 8552 Carbon Fiber Composite, Indian J. Adv. Chem. Sci. 2. 2 (2014) 84–88.

[32] F. Korkees, A. Aldrees, I. Barsoum, D. Alshammari, Functionalised graphene effect on the mechanical and thermal properties of recycled PA6/PA6,6 blends, J. Compos. Mater. 55 (2021) 2211–2224. https://doi.org/10.1177/0021998320987897.

[33] I. Walters, D. Walters, Particles comprising stacked graphene layers, (2019). https://patents.google.com/patent/US20170174520A1/en.

[34] N. Kostoglou, A. Tarat, I. Walters, V. Ryzhkov, C. Tampaxis, G. Charalambopoulou, T. Steriotis, C. Mitterer, C. Rebholz, Few-layer graphene-like flakes derived by plasma treatment: A potential material for hydrogen adsorption and storage, Microporous Mesoporous Mater. 225 (2016) 482–487. https://doi.org/10.1016/j.micromeso.2016.01.027.

[35] G. Höflinger, Leica Microsystems, Brief Introduction to Coating Technology for Electron Microscopy, Appl. Lett. April 2013. (2013) 1–5. https://www.leica-microsystems.com/science-

lab/brief-introduction-to-coating-technology-for-electron-microscopy/.

[36] O. Starkova, S. Chandrasekaran, L.A.S.A. Prado, F. Tölle, R. Mülhaupt, K. Schulte, Hydrothermally resistant thermally reduced graphene oxide and multi-wall carbon nanotube based epoxy nanocomposites, Polym. Degrad. Stab. 98 (2013) 519–526. https://doi.org/10.1016/j.polymdegradstab.2012.12.005.

[37] O. Starkova, S.T. Buschhorn, E. Mannov, K. Schulte, A. Aniskevich, Water transport in epoxy/MWCNT composites, Eur. Polym. J. 49 (2013) 2138–2148. https://doi.org/10.1016/j.eurpolymj.2013.05.010.

[38] F. Korkees, C. Arnold, S. Alston, An investigation of the long-term water uptake behavior and mechanisms of carbon fiber/977-2 epoxy composites, Polym. Eng. Sci. 58 (2018) 2175–2184. https://doi.org/10.1002/pen.24830.

[39] X. Qian, Y.G. Zhang, X.F. Wang, Y.J. Heng, J.H. Zhi, Effect of carbon fiber surface functionality on the moisture absorption behavior of carbon fiber/epoxy resin composites, Surf. Interface Anal. 48 (2016) 1271–1277. https://doi.org/10.1002/sia.6031.

[40] V.M. Karbhari, G. Xian, Hygrothermal effects on high VF pultruded unidirectional carbon/epoxy composites: Moisture uptake, Compos. Part B Eng. 40 (2009) 41–49. https://doi.org/10.1016/j.compositesb.2008.07.003.

[41] S.G. Prolongo, M.R. Gude, A. Ureña, Water uptake of epoxy composites reinforced with carbon nanofillers, Compos. Part A Appl. Sci. Manuf. 43 (2012) 2169–2175. https://doi.org/10.1016/j.compositesa.2012.07.014.

[42] L.R. Bao, A.F. Yee, Effect of temperature on moisture absorption in a bismaleimide resin and its carbon fiber composites, Polymer (Guildf). 43 (2002) 3987–3997. https://doi.org/10.1016/S0032-3861(02)00189-1.

[43] P. Sun, Y. Zhao, Y. Luo, L. Sun, Effect of temperature and cyclic hygrothermal aging on the

interlaminar shear strength of carbon fiber/bismaleimide (BMI) composite, Mater. Des. 32 (2011) 4341–4347. https://doi.org/10.1016/j.matdes.2011.04.007.

[44] G. Keledi, J. Hári, B. Pukánszky, Polymer nanocomposites: Structure, interaction, and functionality, Nanoscale. 4 (2012) 1919–1938. https://doi.org/10.1039/c2nr11442a.

[45] Epotek, Tg - Glass Transition Temperature for Epoxies. Tech Tip 23, (n.d.).

[46] W.J. Cantwell, J. Morton, The impact resistance of composite materials - a review, Composites. 22 (1991) 347–362. https://doi.org/10.1016/0010-4361(91)90549-V.

[47] A. Ghasemi-Kahrizsangi, J. Neshati, H. Shariatpanahi, E. Akbarinezhad, Improving the UV degradation resistance of epoxy coatings using modified carbon black nanoparticles, Prog. Org. Coatings. 85 (2015) 199–207. https://doi.org/10.1016/j.porgcoat.2015.04.011.

[48] R. Karthicksundar, B. Rajendran, P.K. Dinesh Kumar, S. Devaganesh, Thermal characterization of carbon nanoparticle infused GFRP using dynamic mechanical analyzer, Mater. Res. Express. 6 (2019). https://doi.org/10.1088/2053-1591/ab374b.

[49] N. Nuraje, S.I. Khan, H. Misak, R. Asmatulu, The Addition of Graphene to Polymer Coatings for Improved Weathering, ISRN Polym. Sci. 2013 (2013) 1–8. https://doi.org/10.1155/2013/514617.

[50] S. Satheeskumar, G. Kanagaraj, Experimental investigation on tribological behaviours of PA6, PA6-reinforced Al2O3 and PA6-reinforced graphite polymer composites, Bull. Mater. Sci. 39 (2016) 1467–1481. https://doi.org/10.1007/s12034-016-1296-6.

[51] F. Wang, L.T. Drzal, Y. Qin, Z. Huang, Mechanical properties and thermal conductivity of graphene nanoplatelet/epoxy composites, J. Mater. Sci. 50 (2015) 1082–1093. https://doi.org/10.1007/s10853-014-8665-6.